ISBN: 978-3-95450-214-1 ISSN: 2673-5490 doi:10.18429/JACoW-IPAC2021-TUPAB143

LASER PULSE DYNAMICS IN THE SELF-MODULATED REGIME

R. P. Nunes*, UFRGS, Porto Alegre, Brasil
A. Bonatto, UFSCPA, Porto Alegre, Brasil
E. P. Maldonado, ITA, São José dos Campos, Brasil
R. E. Samad, N. D. Vieira Jr, IPEN/CNEN, São Paulo, Brasil

Abstract

In this work, particle-in-cell simulations were carried out to investigate the dynamics of a laser pulse propagating along a H_2 gas jet. The laser-driven wakefield and the density of ionized electrons are analyzed during the pulse propagation through the gas jet. The laser and plasma quantities were chosen in order to have the system operating in the self-modulated regime. Results show how the self-modulation fragments the laser pulse, originating higher-amplitude pulses that can induce bubble formation with wave-breaking and particle injection.

INTRODUCTION

It is well-known that beam physics is a branch of science that suffered a great development along the past decades [1]. The first particle accelerator was built almost 100 years ago, producing 50 keV ion beams inside an accelerating structure with length of approximately a meter [2]. From then to nowadays, not only the energy but also the charge of the accelerated beams increased. The increase in charge was achieved with a better understanding, and consequently the development of the theory associated with the space-charge forces, giving rise to what is known today as beam dynamics. In the other hand, the increase in energy, for many decades, was dependant on the technological advances, always consisting in producing stronger radio-frequency (RF) cavities with smaller thermal losses.

The accelerating structures based on RF cavities are limited to produce electric fields around 100 MV/m [3]. In this way, for generating beams with higher energies, longer machines have to be constructed. This paradigm was broken with the development of the plasma-based accelerating structures [4]. In this technique, a strong perturbation is induced in a plasma, causing charge displacements that propagate as a density wave. This strong plasma-wave produces high-amplitude electric fields, or wakefields, in the order of GV/cm, opening the horizon for higher energetic beams produced within centimeter-long accelerating structures [5]. Once the perturbation is usually produced by a laser pulse, these laser-wakefield accelerators (LWFA) allowed for the production of ~nC beams with ~GeV energies in smaller and less complex machines [6].

Conventional accelerators were often used for scientific purposes, and for some specific applications. However, the possibility of building smaller machines with the plasma-based technique broadened the range of possible applications. Among many, it is possible to cite X-ray and γ-ray sources for use in biomedical applications, physics, and materials science [7]. In addition, the accelerated beams by these machines may be an interesting alternative for the production of radioisotopes for medical purposes [8, 9].

The purpose of this work is to provide a brief investigation about the effect of the self-modulation phenomena along the propagation of a laser pulse in a trapezoidal-shape gas jet. This investigation is carried out with the aid of particle-in-cell (PIC) simulations. The next section presents the results and a brief discussion. The last section summarizes the preliminary conclusions.

SIMULATION RESULTS

The investigated system consists of a laser pulse impinging in a H_2 gas jet target with a trapezoidal-like profile in the longitudinal direction, and a uniform profile in the radial direction. The laser has a Gaussian profile, with waist $w_0 = 7\,\mu m$, and extension $c\tau = 15\,\mu m$. The laser power is 2 TW, and its wavelength is 800 nm. The corresponding dimensionless laser vector potential amplitude, or laser strength, is $a_0 \cong 1.1$. The gas jet consists of an up ramp, with length 80 µm, a plateau of 40 µm, and a down ramp, with a length of 80 µm as well. The gas jet density in the plateau is $n_0 \cong 2{\times}10^{26}$ atoms/m^3, and the laser is focused at the middle of the up ramp.

The simulations presented in this work were carried out by using the FBPIC code [10]. FBPIC is a PIC code for simulating relativistic plasma systems. It is especially suitable for physical simulations of laser wakefield acceleration. FBPIC uses a spectral cylindrical representation, which allows for performing accurate quasi-3D simulations in a reasonable time. Three azimuthal modes were used in the representation. The axial resolution was 1/30 of the laser wavelength. The radial resolution used was 1/60 of the laser waist after self-focusing. A window with length of 100 µm is employed for following the laser pulse along the gas jet. However, all the figures presented in this work use a smaller domain, 50 µm, for better depicting the details of the regions under discussion.

As the laser pulse propagates, the gas jet is ionized, forming a plasma. The laser starts then to interact with the plasma in a process known as self-modulation [5]. Figure 1 illustrates this process after $s = 100.3\,\mu m$ of propagation. In this figure, the axial E_z (in black) and transversal wakefield $W_\perp$ (in blue), both rescaled by the cold nonrelativistic wave-breaking amplitude E_0, are plotted together with the envelope of the dimensionless laser vector potential $a = eA/\omega_0 m_e c$ (in red), in which e is the electron charge,

* roger.pizzato@ufrgs.br

Content from this work may be used under the terms of the CC BY 3.0 licence (© 2021). Any distribution of this work must maintain attribution to the author(s), title of the work, publisher, and DOI

ISBN: 978-3-95450-214-1 ISSN: 2673-5490 doi:10.18429/JACoW-IPAC2021-TUPAB143

Content from this work may be used under the terms of the CC BY 3.0 licence (© 2021). Any distribution of this work must maintain attribution to the author(s), title of the work, publisher, and DOI

A is the laser vector potential, ω_0 is the angular plasma frequency calculated at the gas jet density plateau, m_e is electron mass, and c is velocity of light in vacuum. All previous quantities are analyzed along the co-moving coordinate $\xi = z - s$, in which z is the axial coordinate, and s the propagated distance. Note that the laser profile presents fluctuations in its envelope which are syncronized with the ones found in the wakefields, evidencing the self-modulation phenomena. In addition, peaks in the dimensionless laser envelope match the wakefield peaks.

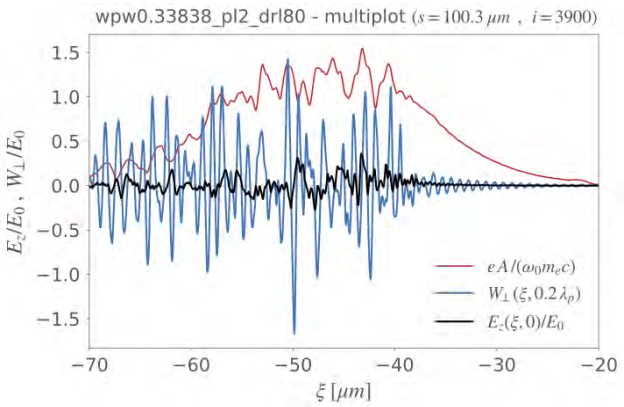

Figure 1: The laser pulse self-modulation after propagating s = 100.3 µm along the gas jet.

The self-modulation phenomena becomes stronger as the pulse propagates further in the gas jet. Hence, the original laser pulse gets fragmented as it propagates, and these laser fragments begin to individually interact with the plasma. Since these laser fragments are shorter and higher in amplitude, if compared to the initial (non-fragmented) laser pulse, they can generate the conditions required for the bubble regime. Figure 2 shows the laser pulse fragmentation for a propagated distance s = 150.5 µm, right after the beginning of the down ramp (s = 120 µm). By inspecting the wakefields, one can see the nonlinear sawtooth-like aspect, a characteristic of the bubble regime. These bubbles (ionic cavities formed due to electrons depletion) can be seen in Fig. 3, in which the density of electrons in the plasma is shown. There is a well-defined white (null-density of electrons) bubble with a high-density peak of electrons behind.

If the self-modulation is sustained, the bubble seen in Fig. 3 can increase, accumulating more electrons behind, until the breaking of the plasma wave occurs. With the wave-breaking, the electrons accumulated behind are injected inside the bubble. This process is shown in Fig. 4 for s = 156.9 µm. It is possible to see in Fig. 4 that there is now an intense density of plasma electrons inside the bubble. As one can see in Fig. 5, inside the bubble the accelerating wakefield is still strong (look at $\xi = -40$ µm), and it still can realize great work over the injected electrons. In addition, at this point the laser strength is almost 4 times higher than its initial value.

The self-modulation process continues and new bubbles can be formed ahead. Figure 6 presents the electron-plasma

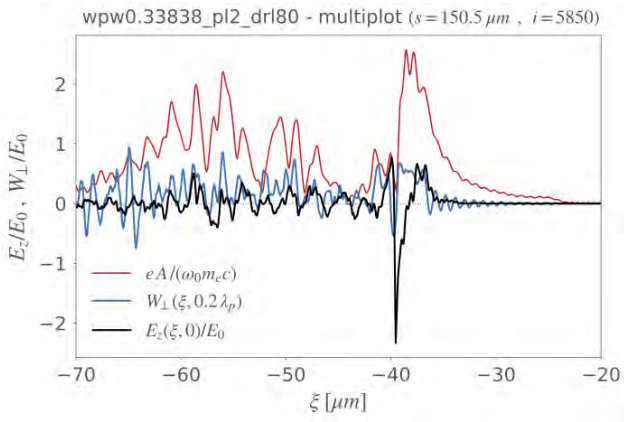

Figure 2: Laser pulse fragmentation after propagating s = 150.5 µm along the gas jet.

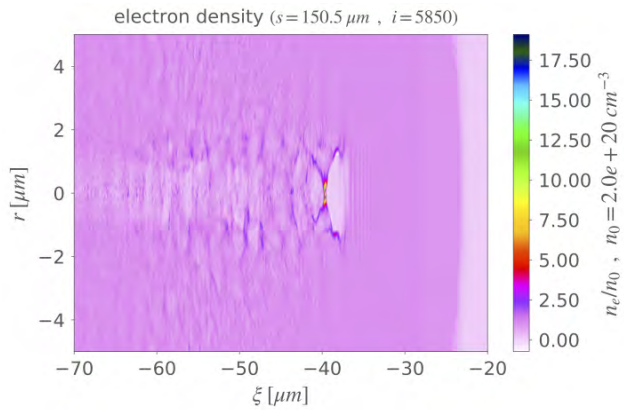

Figure 3: Density of plasma electrons for a propagated distance s = 150.5 µm.

density for s = 177.5 µm. The bubble shown in Fig. 3, in which the electrons were injected, is now in fact the second visible bubble. Figure 7 shows the corresponding laser wakefields at this time. Note that the laser dimensionless amplitude is now smaller, since the gas jet end is near, but still high enough for electron depletion.

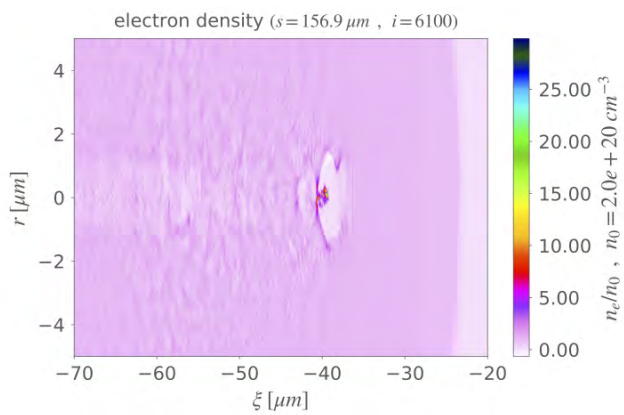

Figure 4: Density of plasma electrons for a propagated distance s = 156.9 µm.

ISBN: 978-3-95450-214-1 ISSN: 2673-5490 doi:10.18429/JACoW-IPAC2021-TUPAB143

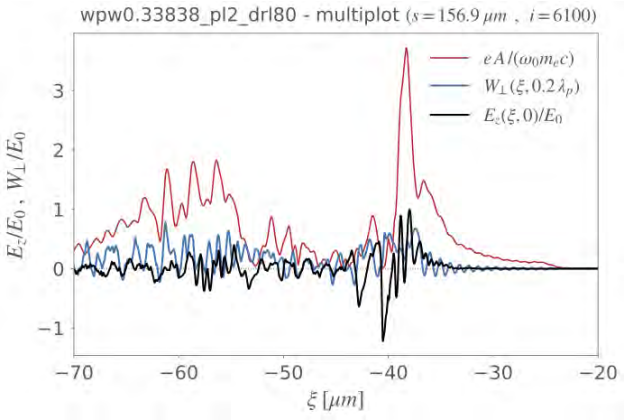

Figure 5: Laser wakefields for $s = 156.9\,\mu m$.

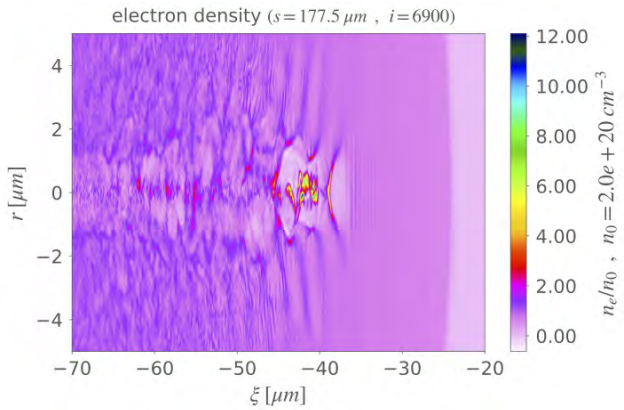

Figure 6: Electron-plasma density for $s = 177.5\,\mu m$.

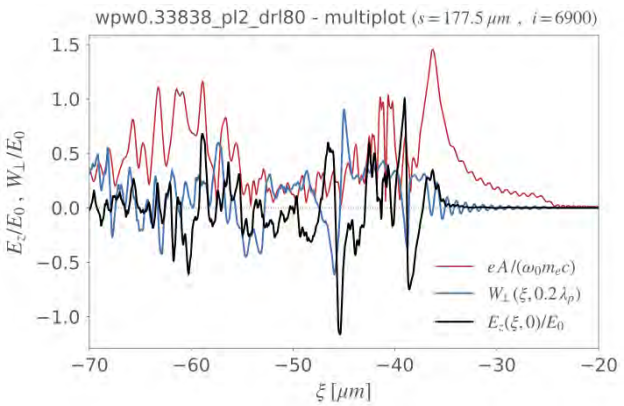

Figure 7: Laser wakefields for $s = 177.5\,\mu m$.

Figure 8 presents the electron-plasma density for $s = 199.4\,\mu m$, right before the laser head exits the gas jet. It is possible to see that the first bubble is empty, with no electrons inside, while the second one is almost destroyed, since it is nearly completely filled by electrons. The presence of this large amount of electrons inside the second bubble changes the longitudinal wakefield E_z, and the previously accelerated electrons now experience decelerating forces. One can see in Fig. 9 that, inside the second bubble ($-50 \lesssim \xi \lesssim -40$), the longitudinal wakefield E_z varies, presenting accelerating and decelerating phases. The result is an intense energy

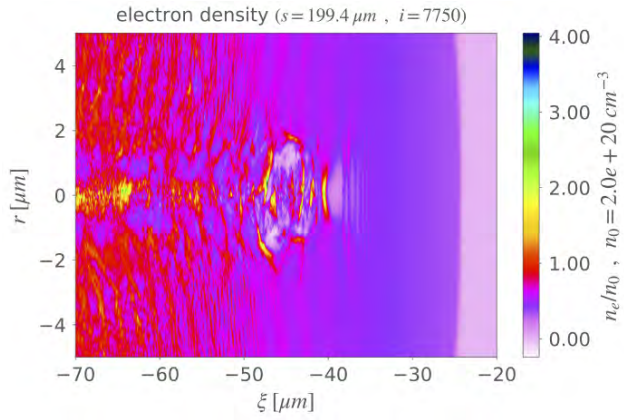

Figure 8: Electron-plasma density for $s = 199.4\,\mu m$.

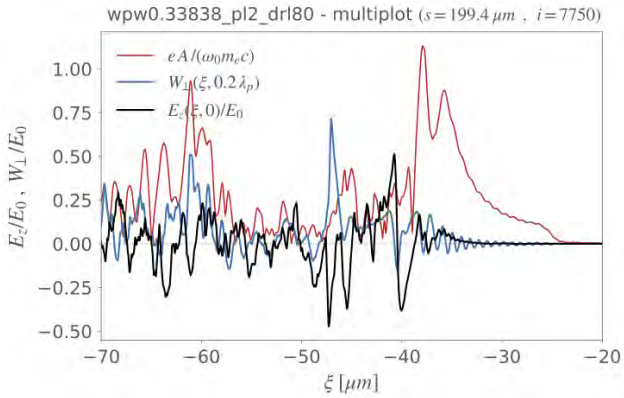

Figure 9: Laser wakefields for $s = 199.4\,\mu m$.

chirp between the electrons that are about to exit the gas jet, forming the accelerated bunch. The laser strength is again almost equal to its initial value.

CONCLUSIONS

In this work, an analysis on the laser pulse propagation along a gas jet was performed. The laser pulse self-modulation is an important process for inducing the bubble regime, electron injection, and consequently bunch formation with a low energy chirp. However, this process has to be ceased adequately, because it can generate new bubbles, which will require new adequate conditions for wave-breaking, particle injection, and acceleration. Otherwise, the output bunch will be a result of acceleration in secondary bubbles, with degraded spatial and energy characteristics. The self-modulation can be can be properly ceased by controlling the down ramp length of the gas jet. In an upcoming work, the accelerated particles will be tracked, in order to quantitatively understand the dynamics of the accelerated particles and the role of the gas jet down ramp length.

ACKNOWLEDGEMENTS

The authors acknowledge the computational support provided by Laboratório Nacional de Computação científica (LNCC), in which the PIC simulations were carried out.

Content from this work may be used under the terms of the CC BY 3.0 licence (© 2021). Any distribution of this work must maintain attribution to the author(s), title of the work, publisher, and DOI

ISBN: 978-3-95450-214-1 ISSN: 2673-5490 doi:10.18429/JACoW-IPAC2021-TUPAB143

Content from this work may be used under the terms of the CC BY 3.0 licence (© 2021). Any distribution of this work must maintain attribution to the author(s), title of the work, publisher, and DOI

REFERENCES

[1] J. B. Rosenzweig, *Introduction to Beam Physics*, New York, NY, USA: Oxford University Press, 2003.

[2] R. Wideröe, "Über ein neues Prinzip zur Herstellung hoher Spannungen", *Archiv für Elektrotechnik*, vol. 21, no. 4, pp. 387-406, July 1928.

[3] E. Esarey, P. Sprangle, J. Krall, and A. Ting, "Overview of plasma-based accelerator concepts", *IEEE Trans. Plasma Sci.*, vol. 24, no. 2, pp. 252-288, Apr. 1996.

[4] T. Tajima and J. M. Dawson, "Laser Electron Accelerator", *Phys. Rev. Lett.*, vol. 43, no. 4, pp. 267-270, Jul. 1979.

[5] E. Esarey, C. B. Schroeder, and W. P. Leemans, "Physics of laser-driven plasma-based electron accelerators", *Rev. Mod. Phys.*, vol. 81, no. 3, pp. 1229-1285, Aug. 2009. doi:10.1103/revmodphys.81.1229

[6] J. P. Couperus *et al.*, "Demonstration of a beam loaded nanocoulomb-class laser wakefield accelerator", *Nature Communications*, vol. 8, no. 1, pp. 487, Sept. 2017. doi:10.1038/s41467-017-00592-7

[7] V. Tomkus *et al.*, "Laser wakefield accelerated electron beams and betatron radiation from multijet gas targets", *Scientific Reports*, vol. 10, no. 1, pp. 16807, Oct. 2020. doi:10.1038/s41598-020-73805-7

[8] A. D. Roberts *et al.*, "Measured bremsstrahlung photonuclear production of 99Mo (99mTc) with 34MeV to 1.7GeV electrons", *Applied Radiation and Isotopes*, vol. 96, pp. 122-128, Feb. 2015. doi:10.1016/j.apradiso.2014.11.008

[9] Z. Sun, "Review: Production of nuclear medicine radioisotopes with ultra-intense lasers", *AIP Advances*, vol. 11, pp. 040701, Apr. 2021. doi:10.1063/5.0042796

[10] R. Lehe, M. Kirchen, I. A. Andriyash, B. B. Godfrey, and J. Vay, "A spectral, quasi-cylindrical and dispersion-free Particle-In-Cell algorithm", *Computer Physics Communications*, vol. 203, pp. 66-82, June 2016. doi:10.1016/j.cpc.2016.02.007